Modelling of second order polynomial surface contacts for programming by human demonstration

Peter Slaets, Wim Meeussen, Herman Bruyninckx, Joris De Schutter
Department of Mechanical Engineering, Katholieke Universiteit Leuven,
Celestijnenlaan 300B, B-3001 Leuven, Belgium.
Email: peter.slaets@mech.kuleuven.be

***Abstract*— This paper presents a contribution to *automatic model building* in *quadratic polynomial* environments, in the context of programming by human demonstration. A human operator moves a demonstration tool equipped with a probe, in contact with an unknown environment. The motion of the demonstration tool is sensed with a 3D camera, and the interaction with the environment is sensed with a force/torque sensor. Both measurements are uncertain, and do not give direct information about the different objects in the environment (such as cylinders, spheres, planes, ...) and their geometric parameters. This paper uses a Bayesian Sequential Monte Carlo method or *particle filter*, to recognize the different discrete objects that form the environment, and simultaneously estimate the continuous geometric parameters of these different quadratic polynomial objects. The result is a complete geometric model of an environment, with different quadratic polynomial objects at its building blocks. The approach has been verified using real world experimental data, in which it is able to recognize three different unknown quadratic polynomial objects, and estimate their geometric parameters.**

***Index Terms*— model building, compliant motion, Bayesian estimation, particle filter, human demonstration, task segmentation, polynomial surfaces**

Fig. 1. Using a demonstration tool equipped with pose and force/torque measurements, a probe makes contact with different quadratic polynomial objects in the environment.

I. Introduction

Compliant motion refers to robot tasks where an object is manipulated in contact with its environment, such as for example an assembly task [1]. One of the challenges in compliant motion is the robust specification of a task, because compliant motion tasks often include many simultaneous contacts and many contact transitions [2]–[4]. Therefore, many task specification methods in compliant motion require a geometric model of the environment where the task will be executed [5]. This paper presents a method to automatically build a geometric model of an environment. While previous work was limited to polyhedral environments in terms of vertices, edges and faces [6], this paper extends the possible building blocks of the environment to quadratic polynomial objects such as spheres, cylinders, ellipsoids, ... While this previous approach was based on multiple Kalman filters (one filter for each possible contact formation), this papers uses a single particle filter. A particle filter can deal with a hybrid (partly discrete and partly continuous) state, and therefore is able to simultaneously distinguish between different discrete quadratic polynomial objects, and estimate the continuous geometric parameters of these polynomials, using only a single filter.

The paper is organized as follows. First Section II presents the definitions of the reference frames together with the demonstration tool which is used to collect sensor data during human demonstration in compliant motion. Section III describes the concept of contact formations with polyhedral objects and the extension to contact formations of a probe with quadratic polynomial objects. The Bayesian interpretation of the sensor data obtained from the demonstration tool is covered in Section IV, where the different environmental objects identified and estimated. Section V describes the real world experiment that validates the presented approach. Finally, Section VI contains conclusions and future work.

II. Definitions

In programming by human demonstration for compliant motion tasks, a human uses a demonstration tool to demonstrate a task in which an object moves in contact with its environment. This demonstration phase however, often requires a geometric environmental model. This paper presents an approach to use the demonstration tool to build a geometric environmental model prior to the task specification phase, based on the sensor measurements of the demonstration tool. These sensor measurements are defined with respect to specific reference frames as discussed in Subsection II-A. Subsection II-B describes the data collection of the wrench and pose sensors mounted on the demonstration tool, and Subsection II-C discusses the unknown geometric parameters and the parameters describing the different discrete objects that can be distinguished in the environment.

A. Frames

The following reference frames (see Figure 2) are considered: $\{w\}$ attached to the world, $\{t\}$ attached to the demonstration tool, $\{c\}$ attached to the contact point and $\{e\}$ attached to the environment object. The position and orientation of a

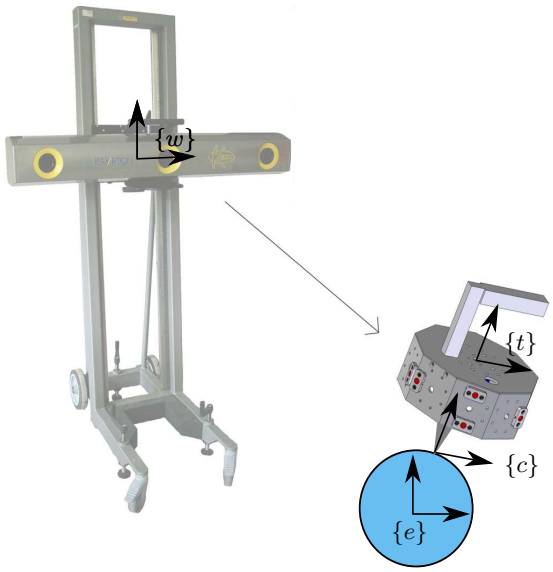

Fig. 2. The reference frame on the camera system $\{w\}$, demonstration tool $\{t\}$, contact point $\{c\}$ and the environmental object $\{e\}$.

reference frame, relative to another reference frame, is called a pose. In this paper a pose is described by a homogeneous transformation matrix (T_a^b), which represents the position and orientation of a reverence frame a relative to a reference frame b:

$$\boldsymbol{P}_a^b = \begin{bmatrix} \boldsymbol{R}_a^b & \boldsymbol{p}_a^b \\ \boldsymbol{0} & 1 \end{bmatrix}, \tag{1}$$

where $\boldsymbol{p}_a^b$ represents the position vector from a to b, and $\boldsymbol{R}_a^b$ represents the orientation matrix between a and b.

B. Demonstration Tool

Figure 1 shows the demonstration tool during the real world experiment. A handle on top of the demonstration tool provides an easy grasp for the human demonstrator to manipulate the demonstration tool and the object attached to it. The demonstration is a hollow cylinder-like shape, consisting of nine faces in 40 $[degrees]$ increments. On each of the faces, up to four LED markers can be mounted. Inside the demonstration tool, a *JR3* wrench sensor is mounted between the demonstration tool and the manipulated object, in order to measure the wrench $\boldsymbol{w}_m$ applied by the human demonstrator to the manipulated object. The wrench measurements are expressed with respect to the $\{t\}$ frame:

$$\boldsymbol{w}_m = \begin{bmatrix} F_x & F_y & F_z & \tau_x & \tau_y & \tau_z \end{bmatrix}^T. \tag{2}$$

where F denotes a linear force, and τ is a moment.

The pose ($\boldsymbol{P}_m$) of the demonstration tool, expressing the position and orientation of the $\{t\}$ frame with respect to the $\{w\}$ frame, is measured indirectly by the Krypton K600 6D optical system (see Figure 2). The K600 system measures the spatial positions of LEDs attached to the demonstration tool at 100 $[Hz]$, with a volumetric accuracy of 90 $[\mu m]$. Rutgeerts e.a. [7] combined the knowledge of the positions of the visible LED markers, to calculate the pose of the demonstration tool, by solving an over-constraint linear system using a least square technique.

C. Unknown geometric parameters

Three types of uncertain geometric parameters are considered in this paper:

- the geometric parameters describing the pose $\boldsymbol{P}_w^e$ of the reference frame $\{e\}$ with respect to the reference frame $\{w\}$
- the geometric parameters describing the polynomial geometry $\boldsymbol{G}_p^e$ of the environmental object with respect to the reference frame $\{e\}$, and
- the geometric parameters describing the position $\boldsymbol{G}_c$ of the contact point.

All these time-invariant parameters are called geometric parameters, denoted by $\boldsymbol{\Theta}$:

$$\boldsymbol{\Theta} = \begin{bmatrix} (\boldsymbol{P}_w^e)^T & (\boldsymbol{G}_p^e)^T & (\boldsymbol{G}_c)^T \end{bmatrix}^T. \tag{3}$$

III. Modelling Polyhedral and Quadratic Polynomial Contact Situations

A general contact model, connecting the measurements of the demonstration tool ($\boldsymbol{P}_m, \boldsymbol{w}_m$) with the unknown geometric parameters ($\boldsymbol{\Theta}$), consists of two types of equations. The first equation relates the manipulated measured object pose ($\boldsymbol{P}_m$) to the geometric parameters ($\boldsymbol{\Theta}$), and is called the *Closure equation*:

$$\boldsymbol{r}_t = h_d(\boldsymbol{\Theta}, \boldsymbol{P}_m) \tag{4}$$

The second equation, called the *consistency based wrench residue equation*, expresses the part of the measured wrench ($\boldsymbol{w}_m$) that is not explained by ideal frictionless contact, as a function of the unknown geometric parameters ($\boldsymbol{\Theta}$) and the measured object pose ($\boldsymbol{P}_m$):

$$\boldsymbol{r}_{6x1} = \begin{bmatrix} \boldsymbol{W}(\boldsymbol{\Theta}, \boldsymbol{P}_m)\phi - \boldsymbol{w}_m \end{bmatrix}^T. \tag{5}$$

The residue should vanish when the wrench measurements and the frictionless contact model are consistent. For a given $\boldsymbol{P}_m$ and discrete object, the first order kinematics are represented by a wrench space $\boldsymbol{W}(\boldsymbol{\Theta}, \boldsymbol{P}_m)$. This wrench space contains all possible wrenches that can be applied between the contacting object at the current pose, and is spanned by the column vectors of $\boldsymbol{W}$. Once a spanning set is selected, every wrench can be represented by a coordinate vector ϕ describing the dependency of the measurement on the spanning set. This coordinate vector is derived using a weighted least square:

$$\phi = \begin{bmatrix} (\boldsymbol{W}(\boldsymbol{\Theta}, \boldsymbol{P}_m))^{\dagger_{\boldsymbol{K}}} \boldsymbol{w}_m \end{bmatrix}^T. \tag{6}$$

The operator $^{\dagger_{\boldsymbol{K}}}$ represents the Moore Penroose weighted pseudo-inverse [8] of a matrix using a weighting matrix $\boldsymbol{K}$,

A. Polyhedral contact situations

1) Contact description: The notion of *principal contacts* (PCs) was introduced in [9] to describe a contact primitive between two surface elements of two polyhedral objects in contact, where a surface element can be a face, an edge or a vertex. Figure 3 shows the six non-degenerate PCs that can be formed between two *polyhedral* objects. Each non-degenerate polyhedral PC is associated with a *contact plane*, defined by a contacting face or the two contacting edges at an edge-edge PC. A general contact state between two objects can be

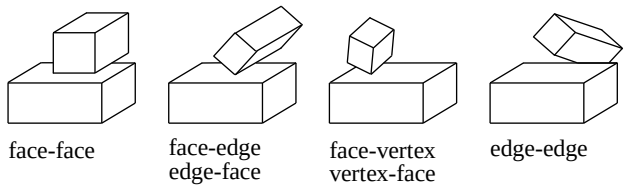

Fig. 3. The six possible non-degenerate principal contacts (PCs) between two polyhedral objects.

characterized topologically by the set of PCs formed, called a *contact formation* (CF). A PC can be decomposed into one

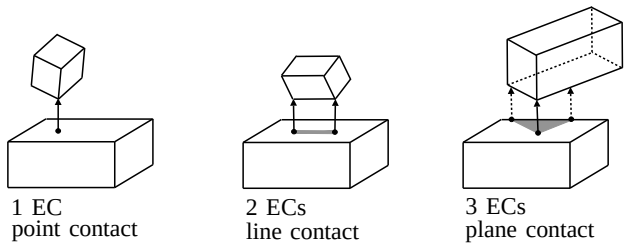

Fig. 4. A principal contact (PC) can be decomposed into one or more elementary contacts (ECs), which are associated with a contact point and a contact normal. The dotted arrows indicate the edge-edge ECs, and the full arrows indicate the vertex-face or face-vertex ECs.

or more *Elementary Contacts* (ECs), providing a lower level description of the CF, as shown in Figure 4. The three types of ECs (face-vertex, vertex-face and edge-edge) are shown in the two examples at the right of Figure 3. The building blocks for polyhedral ECs are a plane, a vertex and an edge. In subsection III-B.2 the ECs are extended to a group of quadratic contacts,leading to additional building blocks: an ellipsoid, a hyperboloid, a cone and a cylinder.

2) Contact modelling: Polyhedral contact models for the different ECs (face-vertex, vertex-face, edge-edge) were derived by Lefebvre [10]. Lefebvre describes each EC contact model by:

- a frame $\{c\}$ on the contact point,
- a wrench spanning set $\boldsymbol{W}$ expressed in this frame, and
- a signed distance function $(\boldsymbol{r}_t)$ between the two contacting polyhedral primitives.

A closure equation (4) and wrench residue equation (5) can be derived for every separate polyhedral EC. For example, a vertex-face contact consists of the parameters of the vertex $(t_p^{t,c})$ expressed in the reference frame $\{t\}$ and the parameters of the face (a normal n_e and a height d) expressed with respect to the reference frame $\{e\}$. To calculate the residue equation, all parameters need to be expressed in the same reference frame. Therefore a transformation between the reference frame $\{t\}$ and the reference frame $\{e\}$ is necessary.

$$ {}_e p^{e,c} = T_e^t(\boldsymbol{P})_t p^{t,c} \tag{7} $$

This transformed vector $({}_e p^{e,c})$ is used to calculate the signed distance function between the vertex and the face, defined by:

$$ \boldsymbol{r}_t = \frac{(n_e)_e^T p^{e,c} - d}{\sqrt{n_e^T n_e}} \tag{8} $$

Similar reasoning is applicable to the wrench spanning set, where a screw transformation [11] is needed to transform $\boldsymbol{W}$ from the $\{e\}$ frame to the $\{t\}$ frame.

$$ \boldsymbol{W}^e(\boldsymbol{\Theta}) = \begin{bmatrix} n_e \\ 0_{3x1} \end{bmatrix}. \tag{9} $$

B. Quadratic contact situations

1) Contact description: In previous research the ECs where described using only three polyhedral building blocks: a vertex, face and an edge. An extension of these building blocks by second order contact surfaces, allows the description of ECs between a vertex and a quadratic polynomial surface [12]. The closed form analytical expression for quadratic polynomial surfaces expressed in a reference frame $\{w\}$, corresponds to a quadratic polynomial equation in three variables:

$$ f(\boldsymbol{X}) = \boldsymbol{X}^T \Delta \boldsymbol{X} + 2C^T \boldsymbol{X} + a_{44} = 0 \tag{10} $$

where Δ is a symmetric 3×3 parametric matrix , $\boldsymbol{X}$ represents the contact point expressed in a $\{w\}$ reference frame and C is a vector of parameters.

Equation (10) is reduced to a standard minimal form by proper choice of a new reference frame $\{e\}$. A standard minimal description leads to an easier classification and parameterization of the different surfaces. The transformation of the reference frame consist of a translational part $(\boldsymbol{p}_e^w)$ and a rotational part $(\boldsymbol{R}_e^w)$. The translation of the $\{w\}$ frame to the center of the polynomial results in the disappearance of the linear term C in equation (10). The rotation of the reference frame results in diagonal matrix Δ only if the rotation matrix $(\boldsymbol{R}_e^w)$ satisfies following constraint:

$$ \Lambda = (\boldsymbol{R}_e^w)^{-1}\Delta(\boldsymbol{R}_e^w) = (\boldsymbol{R}_e^w)^T\Delta(\boldsymbol{R}_e^w). \tag{11} $$

The resulting transformation $(\boldsymbol{P}_e^w)$ reduces the polynomial equation (10) to a simplified quadratic form:

$$ \boldsymbol{X}' = {}_e^w T \boldsymbol{X} \tag{12} $$

$$ f(\boldsymbol{X}') = \boldsymbol{X}'^T \Lambda \boldsymbol{X}' + \delta = 0 \tag{13} $$

with α, β, γ the diagonal elements of Λ. The geometric parameters $(\boldsymbol{G}_p^e)$ describing a vertex-polynomial contact are:

- six parameters $(\boldsymbol{P}_e^w)$ representing the transformation of the reference frame from $\{w\}$ to $\{e\}$;
- four parameters $([\alpha\ \beta\ \gamma\ \delta])$ representing the polynomial object ;
- three parameters representing the contact point $(\boldsymbol{X}')$.

To reduce the complexity of this model some assumptions where made: (i) only quadratic polynomial having a *finite*

center are considered, therefore the elliptic paraboloid and the hyperbolic paraboloid are omitted; (ii) Only *real surfaces* are considered, therefore all imaginary surfaces are omitted. Taking these assumptions into account equation (12) can be used to represent the six different quadratic surfaces shown in Figure 5.

2) Contact modelling: Like polyhedral contacts models , quadratic polynomial ECs are described by:

- a reference frame $\{t\}$ on the demonstration tool,
- a wrench spanning set $\boldsymbol{W}$ expressed in this frame, and
- a signed distance function($\boldsymbol{r}_t$) between the contact point and the environmental object.

The distance from a point p to a quadratic surface defined by equation (12) is equivalent to the distance from the closest point p_{cl} on the surface to p, where $p - p_{cl}$ is the normal to the surface. Since the surface gradient $\nabla f(p_{cl})$ is also normal to the surface, a first algebraic condition for the closest point is

$$p - p_{cl} = \lambda(\nabla f(p_{cl})) = \lambda(2\Lambda p_{cl}) \quad (14)$$

$$p_{cl} = (I + 2\lambda\Lambda)^{-1} p \quad (15)$$

for some scalar λ and I the identity matrix. A second algebraic condition states that the closest point p_{cl} needs to be a point on the quadratic polynomial surfaces. Substitution of $\boldsymbol{X}'$ by p_{cl} (14) in equation (12) leads to a sixth order polynomial constraint in λ:

$$f_c(\lambda) = ((I + 2\lambda\Lambda^{-1})p)^T \Lambda (I + 2\lambda\Lambda)^{-1} p + d = 0 \quad (16)$$

The smallest root ($\lambda = \lambda_{min}$) that complies with this constraint (16) is computed using the root-finding bisection algorithm [13]. This algorithm converges only linearly, but guarantees convergence. Super-linear methods like Newton-Raphson do not guarantee convergence. The algorithm we apply works by repeatedly dividing an interval in half and selecting the subinterval in which the root exists. A subinterval is determined by $\lambda = 0$ and an outer limit λ_{out}. This outer limit is determined by approximating $f_c(\lambda)$ around $\lambda = 0$ by its most dominant term:

$$f_c(\lambda) \approx \quad (17)$$
$$p_{dom}^T (1 + 2\lambda\Lambda_{dom})^{-1} \Lambda_{dom} (1 + 2\lambda\Lambda_{dom})^{-1} p_{dom} + d$$

with scalar Λ_{dom} an element of the diagonal of Λ and scalar p_{dom} is its corresponding direction coordinate. This second order equation (17) is bounded by

$$\lambda_{out1} = -\frac{1}{2\Lambda_{dom}} \text{ and } \lambda_{out2} = \frac{\sqrt{(\frac{-\lambda_{dom} p_{dom}^2}{d})} - 1}{2\lambda_{dom}}. \quad (18)$$

The resulting bounding box is $[0\ \lambda_{out1}]$ when $f_c(\lambda = 0)$ and λ_{out1} have a different sign, otherwise the bounding box is $[0\ \lambda_{out2}]$.

The Euclidean distance from a point to a polynomial is therefore calculated as follows[1]:

$$r_t(p, p_{cl}) = \lambda_{min} \parallel \nabla f(p_{cl}) \parallel \quad (19)$$

[1]When $d = 0$, λ becomes ∞, substitution into equation (19) and evaluating this limit results in $r_{v-p}(p, p_{cl}) = \parallel p \parallel$

The wrench spanning set for a quadratic polynomial contact is defined by the direction of the normal in the contact point (p_{cl}).

$$\boldsymbol{W}^c(\boldsymbol{\Theta}) = \begin{bmatrix} n = \nabla f(p_{cl}) \\ 0_{3x1} \end{bmatrix} \quad (20)$$

IV. Simultaneous Recognition of Discrete Objects and Estimation of Continuous Geometric Parameters

The identification of the surrounding environment is performed by gathering information ($\boldsymbol{P}_m$,$\boldsymbol{w}_m$) of a human exploring the environment using a demonstration tool. This demonstration can be segmented into a contact sequence with different objects. At each different contact, the same analytical contact constraint applies (equation 16), only the values of the uncertain geometric parameters of the objects involved in the compliant motion task differ. To include non contacting discrete situation, the contact model needs to be extended (see Section IV-A). This results in a parameter space consisting of a discrete parameter representing the different discrete objects ($\mathcal{O}$), including the non contacting state, and a continuous parameter space ($\boldsymbol{\Theta}$) representing the union of subspaces (Ω) corresponding with the geometry of the discrete objects. The estimation problem consists of two connected sub-problems: the recognition of the (discrete) object and the estimation of (continuous) geometric parameters. This simultaneous recognition is performed using a hybrid *Probability Density Function* (PDF), shown in Figure 23. In this paper particle filters [14] are used to implement this hybrid estimation problem due to there ability to cope with multi-modal PDFs. The particle filter algorithm (Section IV-B) updates the hybrid PDF, in a two step procedure. First the system model makes a prediction of the geometric parameters that are related to the different objects. In a second step the measurement model corrects this prediction based on sensor data.

A. Extended Contact Model

The contact model of equations (4) and (5) is extended to detect loss of contact during a demonstration. In equation (4) the wrench measurements are represented by a coordinate vector ϕ describing the dependency of the measurement on the spanning set $\boldsymbol{W}$. If $\boldsymbol{W}$ is orthonormal, then the coordinate vector ϕ is proportional to the applied contact force. Therefore ϕ indicates when a contact is established:

$$P(\mathcal{O}_k = \text{no contact}) = \mathrm{N}(\phi, \mathrm{R}) \quad (21)$$

where $N(\phi, R)$ represents a normal PDF in ϕ with mean 0 and where the covariance R corresponds to the noise on the wrench sensor measurements. The extended contact model (21) together with the previous contact models (4),(5) define the 'likelihood' of a measurement $\boldsymbol{z}_k$, given that the time-invariant continues geometric parameters $\boldsymbol{\theta}$ belong to the subspace Ω_k corresponding with the one-dimensional discrete object $\mathcal{O}_k = j$ at timestep k :

$$P\left(\boldsymbol{z}_k \mid \boldsymbol{\theta} \in \Omega_j, \mathcal{O}_k = j\right). \quad (22)$$

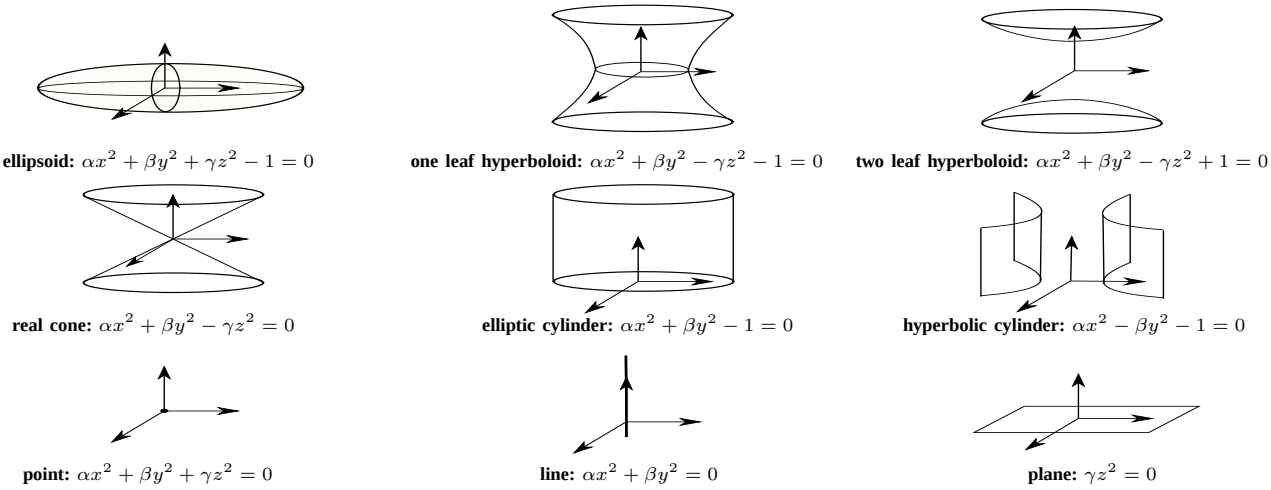

Fig. 5. An overview of the Euclidean classification of real quadratic surfaces having a finite center. The parameters α,β,γ are real and positive, δ equals -1, 0 or 1.

The result of the estimation process is a hybrid PDF expressing the believe that the demonstrator is in contact with the environment (or not) ($\mathcal{O}$) is quantified together with the estimation of the geometric parameters ($\boldsymbol{\theta}$).

$$P\left(\boldsymbol{\Theta} = \boldsymbol{\theta}, \mathcal{O}_k = j \mid \boldsymbol{Z}_{1\ldots k} = \boldsymbol{z}_{1\ldots k}\right).^2 \tag{23}$$

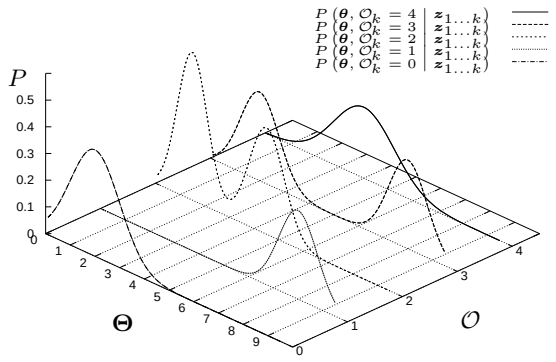

Fig. 6. An example of a probability density function (PDF) of a hybrid joint density, with a one-dimensional continuous geometric parameter $\boldsymbol{\Theta}$ and a one-dimensional discrete state $\mathcal{O}$.

B. Particle filter

The particle filters estimation process consists of a two step procedure: a prediction step followed by a correction step.

1) System model –prediction: A prediction step uses a system model to make a prediction for the hybrid joint density at time step k, given the hybrid joint density at time step $k-1$:

$$P\left(\boldsymbol{\theta}, \mathcal{O}_k = j \mid \boldsymbol{z}_{1\ldots k-1}\right) = \mu P\left(\boldsymbol{\theta}, \mathcal{O}_{k-1} = j \mid \boldsymbol{z}_{1\ldots k-1}\right) + (1-\mu) P_{init}\left(\boldsymbol{\theta}, \mathcal{O}_{k-1} = j\right). \tag{24}$$

[2]In the rest of the paper, the notation $\boldsymbol{A} = \boldsymbol{a}$ is shortened into $\boldsymbol{a}$, wherever the distinction between a stochastic variable and an actual value is unambiguous.

This prediction step states that if there is consistency between the measurements ($\boldsymbol{z}_{1\ldots k-1}$) and the current parameter space ($\boldsymbol{\theta}$), the hybrid PDF is unchanged ($\mu = 1$). Otherwise the estimated PDF is reset to its initial distribution (P_{init}). The consistency indicating parameter is derived by integrating the likelihood of equation (22) over the parameter space $\boldsymbol{\Theta}$ and the state space $\mathcal{O}_k$.

$$\begin{aligned} \mu \quad &= 1 \text{ when } \sum_{\mathrm{j}=1}^{\mathrm{N}} \int \mathrm{P}\left(\boldsymbol{z}_{\mathrm{k}} \mid \boldsymbol{\theta}, \mathcal{O}_{\mathrm{k}} = \mathrm{j}\right) \mathrm{d}\boldsymbol{\theta} > \mathrm{T}_2 \\ \text{else} \quad &\mu = 0 \end{aligned} \tag{25}$$

Where T_2 is a threshold dependent on the dimension of the model equations.

2) Measurement Model – Correction: Every correction step uses the likelihood model to calculate the hybrid joint posterior density over the state and parameter vector at time step k, given the prediction based on the measurements until timestep $k-1$:

$$P\left(\boldsymbol{\theta}, \mathcal{O}_k = j \mid \boldsymbol{z}_{1\ldots k}\right) = P\left(\boldsymbol{z}_k \mid \boldsymbol{\theta}, \mathcal{O}_k = j\right) P\left(\boldsymbol{z}_k \mid \boldsymbol{z}_{1\ldots k-1}\right) P\left(\boldsymbol{\theta}, \mathcal{O}_k = j \mid \boldsymbol{z}_{1\ldots k-1}\right). \tag{26}$$

V. Experiments

This section reports on the real world experiment to validate the presented approach. In the experiment, a human demonstrator manipulates a pin through a sequence of contacts in an environment consisting of different discrete objects: a plane table, a cylinder and a sphere. Figure 1 shows the experimental setup and table 8 shows the chosen uniform uncertainty on the 8-dimensional continuous geometric parameters ($\boldsymbol{\Theta}$) and the definition of the discrete parameter ($\mathcal{O}$). The Gaussian PDF on the wrench residue has a sigma boundary of 3.0 $[N]$ for the forces and 0.33 $[Nm]$ for the torques, while the The Gaussian PDF on the distance at an EC has a sigma boundary of 0.0025 $[m]$. The particle filter uses 80.000 particles, and the joint posterior PDF is dynamically re-sampled using importance sampling, once the effective number of particles drops below 40.000.

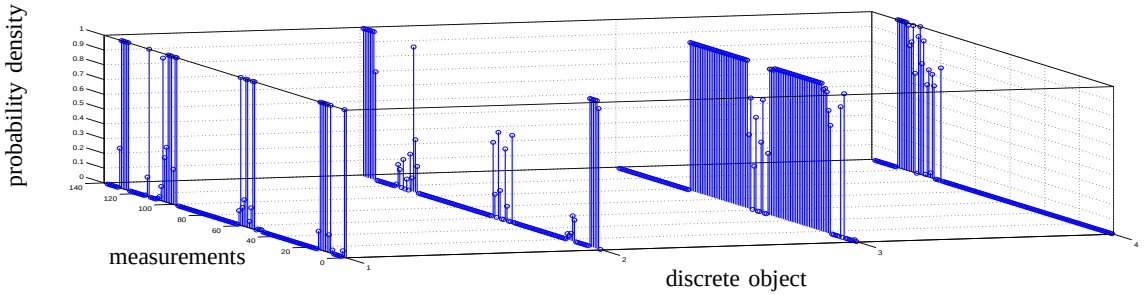

Fig. 7. This figure shows the evolution of the estimated probability on each of the four different discrete objects. The shown probabilities are obtained by integrating over the continuous parameters. The time evolution of the different discrete objects is shown in table 8.

parameter	no contact	plane	cylinder	sphere
$(p_x)^e_w$	-	0[mm]	200[mm]	160[mm]
$(p_y)^e_w$	-	0[mm]	0[mm]	160[mm]
$(p_z)^e_w$	-	160[mm]	200[mm]	160[mm]
$(\theta_x)^e_w$	-	0.2[rad]	0.2[rad]	0[rad]
$(\theta_y)^e_w$	-	0.2[rad]	0[rad]	0[rad]
$(\theta_z)^e_w$	-	0[rad]	0.2[rad]	0[rad]
$r = \sqrt{d}$	-	0[mm]	100[mm]	100[mm]
$(p_z)^c$	-	100[mm]	100[mm]	100[mm]
$\mathcal{O}$	1	2	3	4

Fig. 8. The uniform uncertainty of continuous state parameters are defined in the first 8 rows. The discrete parameters $\mathcal{O}$ is related to four 'contact' situations: no contact, plane, cylinder, sphere.

A. Sequence of Contact Formations

Figure 7 shows the evolution of the estimated probability on each of the four different discrete objects (no contact, plane contact, cylinder contact and sphere contact). Each discrete object is represented by the value of the discrete state as indicated in table 8, and its probability is obtained by integrating over the continuous parameter. The demonstrator subsequently makes contact with a plane, a cylinder, a sphere and then returns in contact with the initial plane. These contact situations are interrupted by non contacting situations. During most of the experiment, the particle filters assign the highest probability to the discrete object that corresponds to the objects that is touched with the demonstration tool. At some points during the experiment, a (false) contact loss is detected because the contact force became too low.

VI. Conclusions

This paper present an extension of the polyhedral contact modelling to second order curvatures represented by a polynomial equation. Because the extended model is non-implicit and non-linear stochastical linear filtering techniques like Kalman filters, e.a. are the wrong tools. A particle filter, which uses a discrete sampled representation of a PDF, overcomes these problems and further makes it possible to compare the probability of different discrete objects. Future work will focus on the extension of the particle to cope with even larger uncertainties by taking 100 times more samples at a reasonable timing cost. This acceleration can be achieved by developing more specific hardware to speed up mathematical calculation by manually developing a parallel pipelined hardware implementation on a field-programmable gate array (FPGA).

Acknowledgment

All authors gratefully acknowledge the financial support by K.U.Leuven's Concerted Research Action GOA/05/10.

References

[1] J. De Schutter and H. Van Brussel, "Compliant Motion I, II," *Int. J. Robotics Research*, vol. 7, no. 4, pp. 3–33, Aug 1988.

[2] M. T. Mason, "Compliance and force control for computer controlled manipulators," *IEEE Trans. on Systems, Man, and Cybernetics*, vol. SMC-11, no. 6, pp. 418–432, 1981.

[3] T. Kröger, B. Finkemeyer, M. Heuck, and F. M. Wahl, "Compliant motion programming: The task frame formalism revisited," *J. of Rob. and Mech.*, vol. 3, pp. 1029–1034, 2004.

[4] J. De Schutter, T. De Laet, J. Rutgeerts, W. Decré, R. Smits, E. Aertbeliën, K. Claes, and H. Bruyninckx, "Constraint-based task specification and estimation for sensor-based robot systems in the presence of geometric uncertainty," 2006, conditionnaly accepted.

[5] W. Meeussen, J. Rutgeerts, K. Gadeyne, H. Bruyninckx, and J. De Schutter, "Contact state segmentation using particle filters for programming by human demonstration in compliant motion tasks," *IEEE Trans. Rob*, 2006, in press.

[6] P. Slaets, T. Lefebvre, J. Rutgeerts, H. Bruyninckx, and J. De Schutter, "Incremental building of a polyhedral feature model for programming by human demonstration of force controlled tasks," *IEEE Trans. Rob*, vol. 23, no. 1, pp. 20–33, 2007.

[7] J. Rutgeerts, P. Slaets, F. Schillebeeckx, W. Meeussen, B. Stallaert, P. Princen, T. Lefebvre, H. Bruyninckx, and J. De Schutter, "A demonstration tool with Kalman Filter data processing for robot programming by human demonstration," in *Proc. IEEE/RSJ Int. Conf. Int. Robots and Systems*, Edmonton, Canada, 2005, pp. 3918–3923.

[8] K. L. Doty, C. Melchiorri, and C. Bonivento, "A theory of generalized inverses applied to robotics," *Int. J. Robotics Research*, vol. 12, no. 1, pp. 1–19, 1993.

[9] J. Xiao, "Automatic determination of topological contacts in the presence of sensing uncertainty," in *Int. Conf. Robotics and Automation*, Atlanta, GA, 1993, pp. 65–70.

[10] T. Lefebvre, "Contact modelling, parameter identification and task planning for autonomous compliant motion using elementary contacts," Ph.D. dissertation, Dept. Mech. Eng., Katholieke Univ. Leuven, Belgium, May 2003.

[11] J. A. Parkin, "Co-ordinate transformations of screws with applications to screw systems and finite twists," *Mechanism and Machine Theory*, vol. 25, no. 6, pp. 689–699, 1990.

[12] P. Tang and J. Xiao, "Generation of point-contact state space between strictly curved objects," in *RSS*, Cambridge, USA, June 2006, pp. 31–38.

[13] R. P. Brent, *Algorithms for minimization without derivatives*. Englewood Cliffs, NJ: Prentice-Hall, 1973.

[14] A. Doucet, N. J. Gordon, and V. Krishnamurthy, "Particle Filters for State Estimation of Jump Markov Linear Systems," *IEEE Trans. Signal Processing*, vol. 49, no. 3, pp. 613–624, march 2001.